FINAL REPORT

to

AIR FORCE OFFICE OF SCIENTIFIC RESEARCH
Project Manager: Dr. A. H. Rosenstein

Grant No. AFOSR 76-2928

CREEP-FATIGUE ENVIRONMENT INTERACTIONS IN SUPERALLOYS

Principal Investigator

Regis M. Pelloux
Professor of Materials Engineering
Department of Materials Science and Engineering
Massachusetts Institute of Technology
Cambridge, MA 02139

April 1981

UNCLASSIFIED

SECURITY CLASSIFICATION OF THIS PAGE (When Data Entered)

REPORT DOCUMENTATION PAGE	READ INSTRUCTIONS BEFORE COMPLETING FORM
1. REPORT NUMBER AFOSR-TR- 81-0450	2. GOVT ACCESSION NO. AD-A098 790
	3. RECIPIENT'S CATALOG NUMBER (9)
4. TITLE (and Subtitle) Creep-Fatigue Environment Interactions in Superalloys,	5. TYPE OF REPORT & PERIOD COVERED Final Report 1 Dec 75 - 12/1/75 - 11/1/80 1 Nov 80
	6. PERFORMING ORG. REPORT NUMBER
7. AUTHOR(s) (10) Regis M. Pelloux	8. CONTRACT OR GRANT NUMBER(s) (15) AFOSR-76-2928 new
9. PERFORMING ORGANIZATION NAME AND ADDRESS Dept. of Materials Science & Engineering Massachusetts Institute of Technology Cambridge, MA 02139	10. PROGRAM ELEMENT, PROJECT, TASK AREA & WORK UNIT NUMBERS 61102F (16) 2306/A2
11. CONTROLLING OFFICE NAME AND ADDRESS AFOSR/NE Bolling AFB, DC 20332	12. REPORT DATE (11) 15 Apr 81
	13. NUMBER OF PAGES 34 (12) 35
14. MONITORING AGENCY NAME & ADDRESS (if different from Controlling Office)	15. SECURITY CLASS. (of this report) unclassified
	15a. DECLASSIFICATION/DOWNGRADING SCHEDULE

16. DISTRIBUTION STATEMENT (of this Report)

Approved for public release; distribution unlimited.

17. DISTRIBUTION STATEMENT (of the abstract entered in Block 20, if different from Report)

18. SUPPLEMENTARY NOTES

19. KEY WORDS (Continue on reverse side if necessary and identify by block number)

fatigue, creep, crack growth, nickel base superalloys, Waspaloy, Astroloy, IN 100, creep-fatigue-environment interactions, micromechanisms of fracture.

20. ABSTRACT (Continue on reverse side if necessary and identify by block number)

The fatigue-creep-environment interactions in nickel base superalloys were investigated from 650°C to 760°C in the low cycle fatigue range and in the crack growth mode as a function alloy chemistry and microstructure.

Three alloys, conventionally cast and forged Waspaloy, powder metallurgy as-hot isostatically pressed low carbon Astroloy, and powder metallurgy superplastically forged IN-100 were compared by room and elevated temperature

DD FORM 1 JAN 73 1473 EDITION OF 1 NOV 65 IS OBSOLETE

UNCLASSIFIED

SECURITY CLASSIFICATION OF THIS PAGE (When Data Entered)

CONTENTS

ABSTRACT

The fatigue-creep-environment interactions in nickel base superalloys were investigated from 650°C to 760°C in the low cycle fatigue range and in the crack growth mode as a function alloy chemistry and microstructure.

Three alloys, conventionally cast and forged Waspaloy, powder metallurgy as-hot isostatically pressed low carbon Astroloy, and powder metallurgy superplastically forged IN-100 were compared by room and elevated temperature low cycle fatigue testing under control of total strain range. It was found that at 427°C and 649°C Waspaloy had the longest fatigue lifetimes followed by low carbon Astroloy, then IN-100, but IN-100 had the highest cyclic flow stress and Waspaloy the lowest.

On the basis of its relatively good combination of fatigue properties, homogenity and isotropy resulting from powder processing, and because it can be heat treated to a wide variety of different microstructures, one alloy, low carbon Astroloy, was selected for a program to systematically determine the effects of changes in microstructure on elevated temperature fatigue behavior. Low carbon Astroloy was heat treated to four very different microstructures with various combinations of fine (500Å) and coarse (2000-8000Å) matrix (γ') and grain boundaries with and without carbides and primary (γ').

Microstructure I in low carbon Astroloy, which is known to offer the best combination of tensile strength and stress rupture properties, was shown here to have the best intermediate and elevated temperature low cycle fatigue strength.

The rates of fatigue crack growth and of creep crack growth were measured in L/C Astroloy in the range of temperatures from 650°C (.64 T_m) to 760°C (.76 T_m). The fatigue crack growth rates are strongly frequency dependent from 10 Hz to 10^{-3} Hz (1 cycle/15 min.). Decreasing frequency promotes intergranular creep cavitation during cyclic loading. At very low frequencies, fatigue crack propagation is completely intergranular, and the cyclic crack growth rates are essentially equivalent to the creep crack growth rates.

Creep crack growth in low carbon Astroloy proceeds in a creep-brittle manner in the range of temperatures from .64 T_m to .76 T_m and in the range of nominal stress from .4σ_y to .7σ_y. Creep crack growth occurs by a process of nucleation and growth of cavities ahead of the crack tip. The kinetics of cavity growth is controlled by power law creep deformation.

Oxidation at the crack tip contributes to the creep crack growth rates in the low temperature range (650°C), where the crack growth rates are small. In the high temperature range (760°C), the acceleration of creep crack growth due to oxidation is negligible. Fractography showed that the role played by oxidation is to enhance creep cavitation.

The results of sequential fatigue-creep cracking periods demonstrated that a simplistic linear superposition damage rule cannot be used to predict the crack growth rates under combined fatigue-creep loading. The fatigue crack growth rates at a frequency of 1 Hz following a creep loading period are accelerated as much as one order of magnitude. This acceleration of fatigue cracking after creep cracking is attributed to the creep damage in the crack tip region of the creep crack.

I. Introduction

Fatigue damage limits the useful life of nickel-base superalloys in many applications. Today there is considerable emphasis on fatigue in design of gas turbine components. Lack of a good mechanistic understanding of low cycle fatigue and fatigue crack growth causes time consuming, expensive generation of design data before any new alloy system can be used.

The problem of fatigue in nickel-base superalloys is very complex because these alloy systems are used at temperatures from 0.4 to 0.8 T_M. Up to about 0.6 T_M the flow stress of γ' precipitation strengthened superalloys remain constant with increasing temperature, while the ductility and tensile strength show only slight reductions. By contrast the fatigue strength decreases rapidly with temperature, and the fatigue lifetime can be reduced by a factor of twenty from room temperature to 760°C (0.67 T_M). Obviously, fatigue limits the full utilization of the elevated temperature strength of nickel-base superalloys.

It was the intent of this program to further the understanding of the mechanisms of fatigue of superalloys. First, different alloy systems, including Waspaloy, Astroloy and IN-100, ranging in γ' volume fraction from 22 to 56 percent were evaluated and compared by room and elevated temperature low cycle fatigue testing under controlled total strain range. Then on the basis of this investigation, powder processed, as-hot isostatically pressed, low carbon Astroloy was selected for a systematic study of the influence of grain boundary structure and γ'

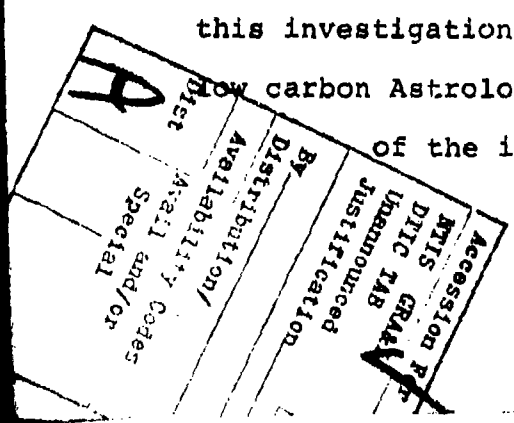

size distribution on room and elevated temperature low cycle fatigue behavior.

The fatigue behavior of the low carbon Astroloy was also of particular interest because of the novel manner in which it was processed. Pre-alloyed low carbon Astroloy powder was consolidated by hot isostatic pressing (HIP) and tested in the as-consolidated condition without benefit of subsequent forging. It is already known that HIP powder metallurgy superalloys exhibit equivalent monotonic properties in comparison with conventionally cast and forged alloys, but the cyclic properties have not yet been fully characterized. It was expected that the homogeneous isostropic structure produced by powder processing might be beneficial to fatigue.

The goals of the research program were:

1. To compare the properties of three different nickel base superalloys used for turbine disk application under elevated temperature low cycle fatigue
2. To compared the LCF properties of apowder metallurgy HIP processed nickel-base superalloy with those of a wrought alloy having similar chemistry.
3. To determine the effects of temperature and frequency on the LCF behavior of a powder processed nickel-base superalloy.
4. To determine the effects on LCF behavior of changes in γ' size and grain boundary structure in a powder processed nickel-base superalloy.

5. To compare the mechanisms of cracking under fully plastic conditions to those under elastic-plastic conditions at similar temperatures and frequencies.

II. Summary of Work

1. Evaluation of LCF properties of three nickel-base Superalloys.

Three nickel-base superalloys currently used for turbine disks were studied during the years year; they were Waspaloy, L/C Astroloy, and IN-100. The Waspaloy alloy was cast and hot worked; the IN-100 alloy was super-plastically forged from an extruded powder metallurgy (P/M) billet, and the Astroloy alloy was as-hot isostatically pressed (HIP) prealloyed powder. The three alloys differ markedly in their volume fractions of the γ' phase. These volume fractions are 22% for Waspaloy, 35% for Astroloy, and 55% for IN-100.

The study of hardening and softening under controlled total strain range is fundamental to fatigue research. At room temperature, the superalloys were found to cyclically harden to a maximum $\Delta\sigma$ at 10 cycles, then cyclically soften until failure. Figure 1 compares the cyclic response of Waspaloy at different strain ranges; it is evident that the maximum stress amplitude is reached at 10 cycles regardless of strain range. The 10 cycle maximum at room temperature is not confined to Waspaloy. In Figure 2 the room temperature cyclic response of Waspaloy, L/C Astroloy, and IN-100 are compared for a strain range of $\Delta\varepsilon_D^T = 2\%$. Again the maximum in stress amplitude is observed at 10 cycles for

all three alloys. This observation is consistent with the work of Wells and Sullivan (1), Merrick (2), Stoltz (3), and Pineau (4).

Hardening may be characterized by the parameter

$$\beta_h = \frac{\Delta\sigma_{max} - \Delta\sigma_1}{\Delta\sigma_1}$$

and softening by the parameter

$$\beta_s = \frac{\Delta\sigma_{max} - \Delta\sigma_{min}}{\Delta\sigma_1}$$

where $\Delta\sigma_1$ is the stress range of the fist cycle and $\Delta\sigma_{min}$ is the minimum stress range observed <u>after</u> the maximum stress range, $\Delta\sigma_{max}$. For Figure 2 the values of β_h, the hardening parameters of Waspaloy, L/C Astroloy and IN-100 are: 0.18, 0.32, and 0.42 respectively. The softening parameters are 0.12, 0.15, and 0.22 respectively. In this case it appears that the amount of hardening and softening is related to the volume fraction of γ' in the alloy.

At elevated temperature the cyclic response of the three superalloys changes. At 800°F, there was no softening in L/C Astroloy or IN-100. At 1200°F, softening was again observed in Waspaloy and L/C Astroloy but curiously not in IN-100. For low low strain ranges, Waspaloy and L/C Astroloy do soften after initial hardening, but this 1200°F behavior differs considerably from behavior at room temperature. At 1200°F the maximum in stress amplitude is not reached until more than 10% of the lifetime to failure has elapsed. These observed differences coupled with the observed absence of softening at 800°F suggest

that the 1200°F phenomenon is mechanistically different from that at room temperature.

Softening complicates the definition of the cyclic stress-strain curve. In most cases the room and elevated temperature cyclic stress-strain curves lie along the monotonic curves; however, at 1200°F softening is great enough at low strain ranges to shift the cyclic stress-strain curve below the monotonic curve.

Figure 3 shows that fatigue lifetime correlates well with total strain range. Lines drawn through both total strain range and plastic strain range points should extrapolate back to the same intercept at 1/2 cycle called the "fatigue ductility coefficient" which corresponds to the monotonic tensile ductility. Since lifetime versus plastic strain does not extrapolate to a realistic fatigue ductility coefficient, total strain range is preferred for lifetime prediction.

Lifetime to failure correlates well with total strain range for all temperatures studied. On this basis Waspaloy has the best fatigue properties, followed in order by Astroloy and IN-100. The ranking is not changed by temperature, but the difference between the alloys seems to increase with temperature.

Figure 3 shows that the relative performance of the three alloys is the same for all strain ranges of interest. As a consequence, it was decided to determine lifetimes as a function of temperature and frequency at one strain range. Results of

such a study with Waspaloy ($\Delta\sigma_L^T$ = 2.2% are plotted in Figure 4. The lifetimes are extremely temperature dependent.

Figure 4 suggest that the fatigue behavior of Waspaloy may be divided into three regimes with the low and high temperature regime being more temperature sensitive than the middle. Study of fractographs and review of the literature suggest that the three regimes correspond to (1) Stage 1 (transgranular crystallographic), (2) Stage II (transgranular non-crystallographic, (3) Intergranular failure. Regimes I and II are frequency insensitive, while Regime III is very frequency sensitive. It is expected that variations in grain boundary structure will affect only the transition temperature from II to III. Variation in γ' size which affect slip character may affect behavior in Regime I and the I to II transition temperature.

2. Low Cycle Fatigue Performance of L/C Astroloy

Low carbon Astroloy was selected as a reference P/M-HIP superalloy for a study on the effects of changes in microstructures on elevated temperature fatigue behavior. Low carbon Astroloy was heat treated to four very different microstructures with various combinations of fine (500Å) and coarse (2000-8000Å) matrix γ' and grain boundaries with and without carbides and primary γ'. Conventional cast and forged Udimet 700, which is similar in chemical composition to Astroloy, was also tested.

The four different microstructures are the result of the heat treatments described in Table I. The characteristic features of the microstructures are sketched in Figure 5. Each microstructure is described as follows:

Microstructure I. The baseline microstructure is characterized by "wavy" grain boundaries containing both primary γ' and $M_{23}C_6$ carbides. The matrix γ' varies in size with three modes in the distribution: 0.8μm, 0.2μm, and 0.04μm.

Microstructure II. This microstructure contains no grain boundary γ' due to solution above the γ' solvus. $M_{23}C_6$ carbides are present in the grain boundaries. The matrix γ' is one size, about 0.2μm.

Microstructure III. In this case there are no carbides in the grain boundaries but solution below the γ' solvus results in some 1 μm grain boundary and some 0.8μm matrix γ'. Oil quenching and single step aging produce fine matrix γ' of 0.05 μm.

Microstructure IV. A slow cool results in no grain boundary carbides and a very broad γ' size distribution. One-half of the 42 per cent γ' is 2 μm or larger.

After room and elevated temperature low cycle fatigue tests, it was found that:

1. At room temperature cyclic hardening following by cyclic softening was observed. Though initial cyclic flow stress depended strongly on γ' size, saturation flow stress did not.

2. At 427°C and 538°C gross discontinuous flow behavior was observed during the first ten cycles of testing. Discontinuous flow was not observed in low carbon Astroloy with predominantly fine 500Å γ'.

3. At 427°C and 538°C fatigue lifetime and mode of crack propagation were related to matrix γ' size. Low carbon Astroloy with only 2000Å γ' had the shortest fatigue lifetimes and exhibited both stage I crack initiation and crack propagation along persistent slip bands. Low carbon Astroloy with the other microstructures which had some fine 500Å γ' had longer fatigue lifetimes and exhibited stage I initiation but stage II propagation.

4. At 649°C and 760°C grain boundary structure influenced fatigue lifetimes. Grain boundaries with both carbides and primary γ' had the longest fatigue lifetimes. Absence of primary γ' and or carbides in the grain boundaries resulted in

transition to intergranular failure and reduced fatigue lifetimes.

5. at 649°C conventionally cast and forged Udimet 700 had shorter fatigue lifetimes than powder processed as-hot isostatically pressed low carbon Astroloy.

6. Microstructure I in low carbon Astroloy, which is known to offer the best combination of tensile strength and stress rupture properties, was shown here to have the best intermediate and elevated temperature low cycle fatigue strength.

Fatigue lifetime of low carbon Astroloy was found to be sensitive to microstructure. In Figure 6 the number of cycles to failure is plotted versus the plastic strain range for LCF tests at 0.05 Hz and 649°C for the four microstructures. Under these test conditions, Microstructure I is the best and Microstructure III the worst. In Figure 7 lifetimes to failure for the four microstructures are plotted versus temperature for a constant total strain range of 2.2%. At room temperature, lifetimes to failure varied even though the saturation plastic strain was the same for each microstructure, suggesting that initial cyclic plastic strain may govern fatigue lifetime. At 427°C and 538°C microstructure II exhibited shorter fatigue lifetimes than the other three microstructures. At 649°C and 760°C microstructures II and III show markedly shorter lifetimes to failure than microstructures I and IV.

Scanning electron microscopy and optical microscopy of surface replicas was conducted on failed LCF specimens to relate differences in fatigue lifetime to modes of fatigue failure. Modes of fatigue crack initiation and propagation for various alloys, microstructures and test conditions are listed in Table II. The predominant mode of failure is stage I crack initiation along persistent slip bands followed by stage II transgranular propagation.

The reduction in fatigue lifetime of microstructure II at 427°C and 538°C was associated with stage I crack propagation along persistent slip bands. Thus, this microstructure which has no fine 500Å γ' apparently results in weaker intense slip bands.

The poor fatigue performance of microstructure III at 649°C and 760°C was associated with intergranular crack initiation and propagation. Microstructure III has no grain boundary $M_{23}C_6$ carbides. Microstructure II also showed intergranular cracking at 649°C and 760°C. Grain boundaries in microstructure II contain $M_{23}C_6$ carbides but no primary γ'. It is concluded that both primary γ' and $M_{23}C_6$ carbides contribute to grain boundary strength in elevated temperature fatigue.

3. Fatigue and Creep Crack Growth in L/C Astroloy.

Following the extensive low cycle fatigue work described in Sections 1 and 2, it was decided to investigate the rates and mechanisms of fatigue and creep crack growth at elevated temperatures in the same alloy. One of the main reasons for this approach was due to the fact that the main problems associated with the new PM/HIP superalloys is the presence of small ceramic particles which act as fatigue and crack crack initiation sites. Consequently, it is important to know the growth rates of cracks growing from these small defects. The effects of temperature, frequency, wave shape and environment were investigated.

A PM/HIP low carbon Astroloy alloy supplied by Pratt and Whitney was used in this investigation. Fatigue and creep crack growth tests were performed with single edge notched bars. The starter notch was 1 mm deep. Shallow side grooves were used in order to maintain a straight crack front during crack growth. For continuous fatigue crack growth, the crack length is measured with a traveling telescope with ± .01 mm accuracy. For sequential fatigue and creep crack growth tests, creep crack growth is measured in macrophotographs. A potential drop technique was used to monitor creep crack growth.

Experimental Results

The fatigue crack growth rates in air at 650°C and

760°C versus the range of the stress intensity factor ΔK are plotted in Figures 8 and 9. The cyclic crack tip opening displacement (CTOD = $\frac{\Delta K^2}{2YE}$) versus ΔK is also plotted. (Y is the yield stress, E is the elastic modulus.) The data covers the range of ΔK from 10 to 100 MPa$\sqrt{m}$. The three regions of the typical da/dn- K curve are not fully represented. The low ΔK region remains to be explored at 650°C at low and high frequencies. In region 2 of the da/dn - ΔK curve the crack growth rate increases with decreasing frequency and increasing hold times. At 760°C the apparent threshold ΔK increases with increasing hold times and the region I slope increases markedly with decreasing frequency.

At high frequencies (10 Hz and 1 Hz) the fracture path was essentially transgranular at 650°C and 760°C. At low ΔK the fracture path is strongly crystallographic which is typical of low growth rates in γ-γ' alloy at high temperatures. As ΔK increases, the fracture path is less crystallographic, although it is still transgranular with well-defined striations. The crack front fans out in each grain indicating a reinitiation process at the crossing of each grain boundary. The striations are strongly crystallographic which is typical of a planar slip process of sliding off and fracture at the crack tip. For the 5.4 min. and 15 min. hold times, the fracture path is completely intergranular.

Figure 10 summarizes the fracture modes in a plot of crack

growth versus frequency for a ΔK value of 50 MPa$\sqrt{m}$. We see that at low frequencies, and long hold times, the crack growth rate per cycle is inversely proportional to the frequency indicating a process of fracture by pure creep crack growth.

Creep Crack Growth Rate Data

Figure 11 shows the results of constant load creep crack growth tests at 650°, 700° and 760°C. The data are plotted as da/dt in m/hour versus K, the stress intensity factor. Although there is a larger scatter band, the data is easily correlated with the K factor at different gross stress levels at least for the single edge notch specimen used here. This correlation is in agreement with other results on creep crack growth in nickel base superalloys. A mathematical analysis of the stress and strain fields at the tip of a sharp crack undergoing creep has been recently given by Riedel and Rice (4). Riedel's analysis shows that the use of K as a correlation parameter for da/dt is justified for high strength, low ductility, creep resistant alloys.

A detailed fractographic investigation of the creep crack growth (CCG) specimens shows a completely intergranular fracture path. The grain boundary facets are not sharply outlined as they are made up of a network of microvoids. The voids are spherical in shape and each void appears to be centered around a second phase particle. There is no indication of elongation of the voids due to a grain boundary

sliding process. There is little or no secondary grain boundary cracking.

Sequential Fatigue and Creep Crack Growth Tests

A series of tests were performed in air and in vacuum to study the interactions between sequential crack front advances due to creep an to fatigue. The tests were conducted in the following manner: 100 to 300 fatigue cycles at 1 Hz were followed by creep crack growth for given hold times. This sequence was repeated until the test bar broke, or until large plasticity effects were observed in the test specimen.

It was found that the creep crack growth rates under sequential periods of fatigue and creep are greater than under conditions of steady creep crack growth. There is a period of accelerated creep crack growth following fatigue cracking. The creep crack growth rate decreases as the crack front advances by creep cracking. At the limit, the crack growth rate reaches the static crack growth rate.

This transient effect of accelerated CCG may be due to the following factors:

> Creep crack growth is accelerated as long as the creep crack is growing through the pre-damaged cyclic plastic zone at the tip of a fatigue crack. This damage may take the form of a high density of dislocations or vacancies or of a high concentration of oxygen atoms which may have been swept into the grain boundaries by dislocation transport. Creep

crack growth is also accelerated because of the high tensile stresses present at the tip of the fatigue crack following cyclic crack growth. It takes a while for the stresses to relax by creep to lead to in a decrease of the CCGR.

In summary, the main results of the crack propagation studies are:

1. The rates of fatigue crack growth and of creep crack growth were measured independently in L/C Astroloy in the range of temperatures from 650°C to 760°C.

2. It was found that the rates of cracking are better correlated with K, the stress intensity factor, than with C* integral.

3. The fatigue crack growth rates are strongly frequency dependent, approaching the pure creep crack growth rate at very low frequencies (<1 cycle / 15 minutes).

4. Sequential fatigue-creep cracking periods demonstrated that a simplistic superposition damage rule cannot be used to predict the crack growth rates. Creep crack growth rates following high frequency (1 Hz) fatigue cycles are an order of magnitude greater than the creep crack growth rates which should be expected from continuous creep cracking.

5. Oxidation effects at the crack tip contribute extensively to the creep crack growth rates in the low temperature range (650°C). At 760°C, the contribution of oxidation to creep crack growth is small compared to the creep cavitation damage.

6. A theoretical model of creep crack growth is proposed based on time dependent analysis of the crack tip stress distribution and on a cavity growth mechanism by power law creep. The model predicts that creep crack growth rates are a strong function of triaxiality ahead of the crack tip. With a plastic constraint factor equal to 2, the model predicts the creep crack growth rates of low carbon Astroloy within a factor of 10 of the experimental data. This model of creep crack growth also predicts that the creep crack growth rate increases with decreasing grain size, decreasing cavity spacing and decreasing threshold cavity nulcation stress.

7. A theoretical prediction of creep crack growth rates was also performed based on the time-dependent crack tip stress field and with the assumption of a diffusive cavity growth mechanism. The prediction overestimated the creep crack growth rates by several orders of magnitude and predicted a wrong temperature dependence for the creep crack growth rates. It is concluded that cavity growth by grain boundary diffusion is suppressed by several orders of magnitude during creep cavitation in low carbon Astroloy.

References

1. C. H. Wells and C. P. Sullivan, Low Cycle Fatigue Damage of Udimet 700 at 1400°F. ASM Transactions. Quart. 58, 391 (1965).

2. H. T. Merrick, The Low Cycle Fatigue of Three Wrought Nickel Base Superalloys, Met. Trans. 5, 891 (1974)

3. R. E. Stoltz, Private communication, MIT, (1975).

4. D. Fournier and A. Pineau, Low Cycle Fatigue of Inconel 718 at 298°K and 823°K, Met. Trans. 8A, (1977).

5. H. Riedel and J. R. Rice, Tensile Cracks in Creeping Solids. ASTM STP 700, p. 112, (1979).

Conclusions

The main achievements of the research work reported here are:

1. Development and refinement of the test procedures used to evaluate low cycle fatigue and fatigue-creep crack growth performance of high strength nickel base superalloys.

2. Detailed evaluation of the role of the intergranular and transgranular microstructures of Astroloy on its performance in low cycle fatigue.

3. Measurements of the fatigue and creep crack growth rates in Astroloy as a function of temperature, frequency, wave shape and hold times.

4. Extensive correlations between the micromechanisms of fracture and the continuum mechanics parameters on the one hand and the alloy microstructure on the other hand.

The following research tasks were identified:

1. A quantitative separation of the initiation and propagation stages is badly needed. A systematic study of the creep fatigue growth of short cracks (< 1 mm) may help resolve this problem.

2. The use of K as a fracture mechanics correlation parameter at elevated temperatures is purely arbitrary, even if the correlation of K with the crack growth rates appear acceptable. The strong time and temperature dependence of elastic stresses at a crack tip make the use of K meaningless. There is need for a detailed analysis of time-dependent stress and strain distributions at the tip of a growing creep crack.

3. A great deal of fundamental work remains to be done to understand the effect of environment on cavitation and cracking at crack tips.

4. The life prediction methodology is at this time purely empirical. There is a need for an integrated life-prediction methodology which can account not only for frequency and wave shape effects, but also for sequential periods of creep and fatigue and for microstructural effects.

Achievements

J. Runkle, Elevated Temperature Fatigue of Nickel Base Superalloys, ScD thesis, MIT, February 1978.

J. S. Huang, Fatigue Crack Growth and Creep Crack Growth of P/M HIP Low Carbon Astroloy at High Temperature. ScD thesis, MIT. February 1981

Publications

J. C. Runkle, R. M. Pelloux, Micromechanisms of Low Cycle Fatigue in Nickel Base Superalloys at Elevated Temperature. ASTM STP 675, Fatigue Mechanisms, 1979. p. 501-527.

J. S. Huang, R. M. Pelloux, Low Cycle Fatigue Crack Propagation In Hastelloy X at 25 and 760°C. Met. Trans. A., Vol. 11A, June 1980, p. 899-904.

R. M. Pelloux, J. S. Huang, Creep-Fatigue-Environment Interactions, Editors, Pelloux, Stoloff, 1980.

J. S. Huang, R. M. Pelloux, Creep Crack Growth in Astroloy: Experimental Data and Theory. In preparation to be submitted to Met. Trans. A.

J. S. Huang, R. M. Pelloux, Effect of Frequency and Temperature on Fatigue Crack Growth in Astroloy, in preparation. To be submitted to Met. Trans. A.

R. M. Pelloux, N. S. Stoloff (RPI) organized an AIME symposium on Creep-Fatigue-Environment Interactions, Fall meeting, AIME, September 18-19, 1979. The proceedings were published by the Metallurgical Society of AIME.

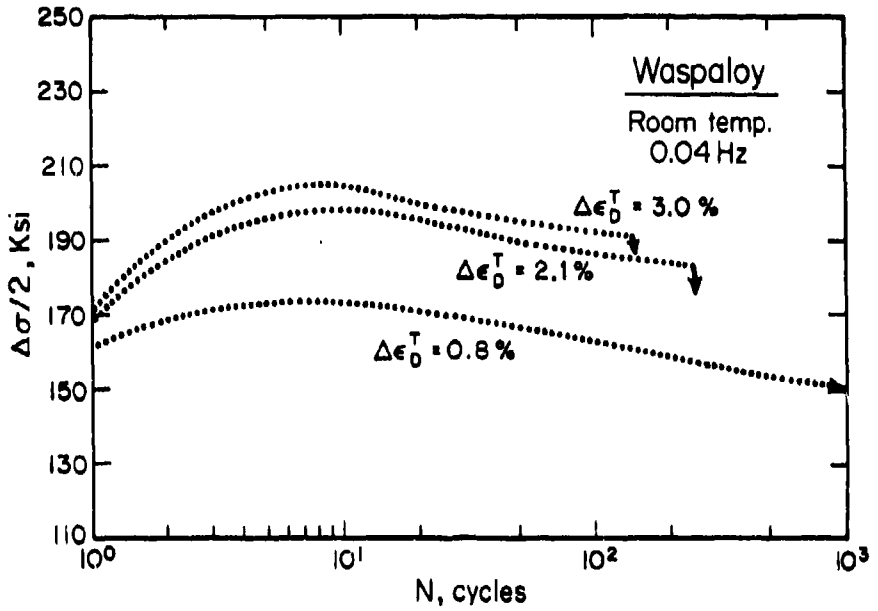

Figure 1 The cyclic response of Waspaloy at room temperature under different strain ranges shows a peak in stress range at about 10 cycles.

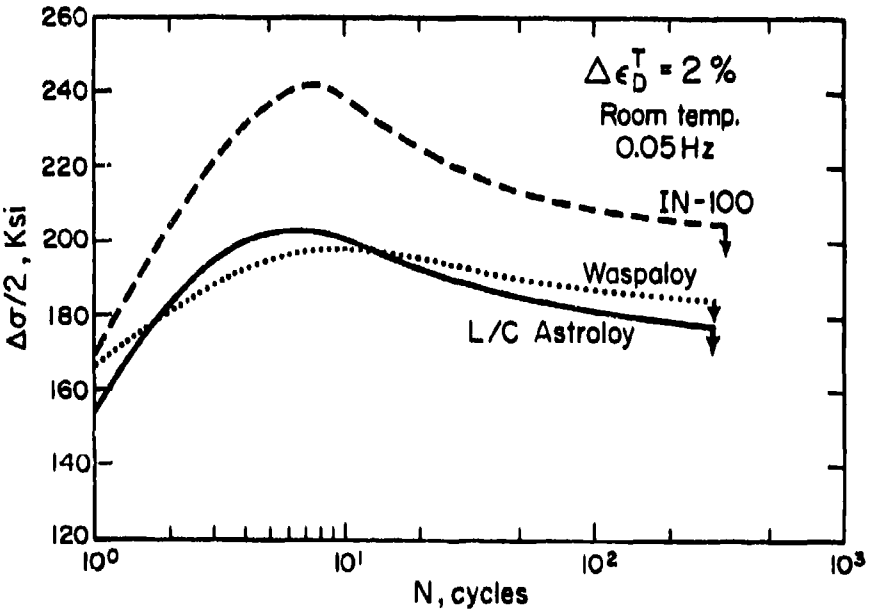

Figure 2 A comparison of the room temperature cyclic response of Waspaloy, L/C Astroloy, and IN-100 at the same strain range shows similar hardening/softening behavior.

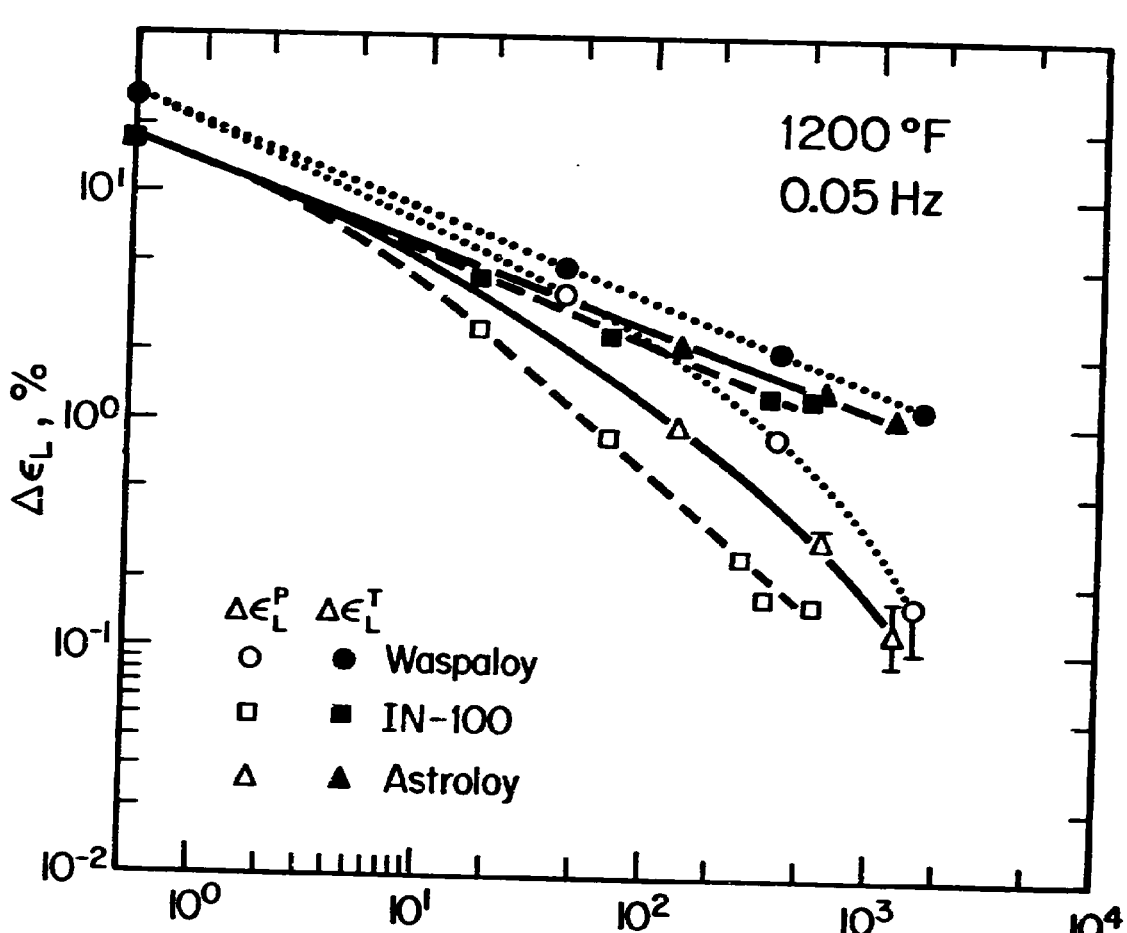

Figure 3. Longitudinal total and plastic strain ranges versus number of cycles to failure for Waspaloy, L/C Astroloy, and IN-100 at 1200°F.

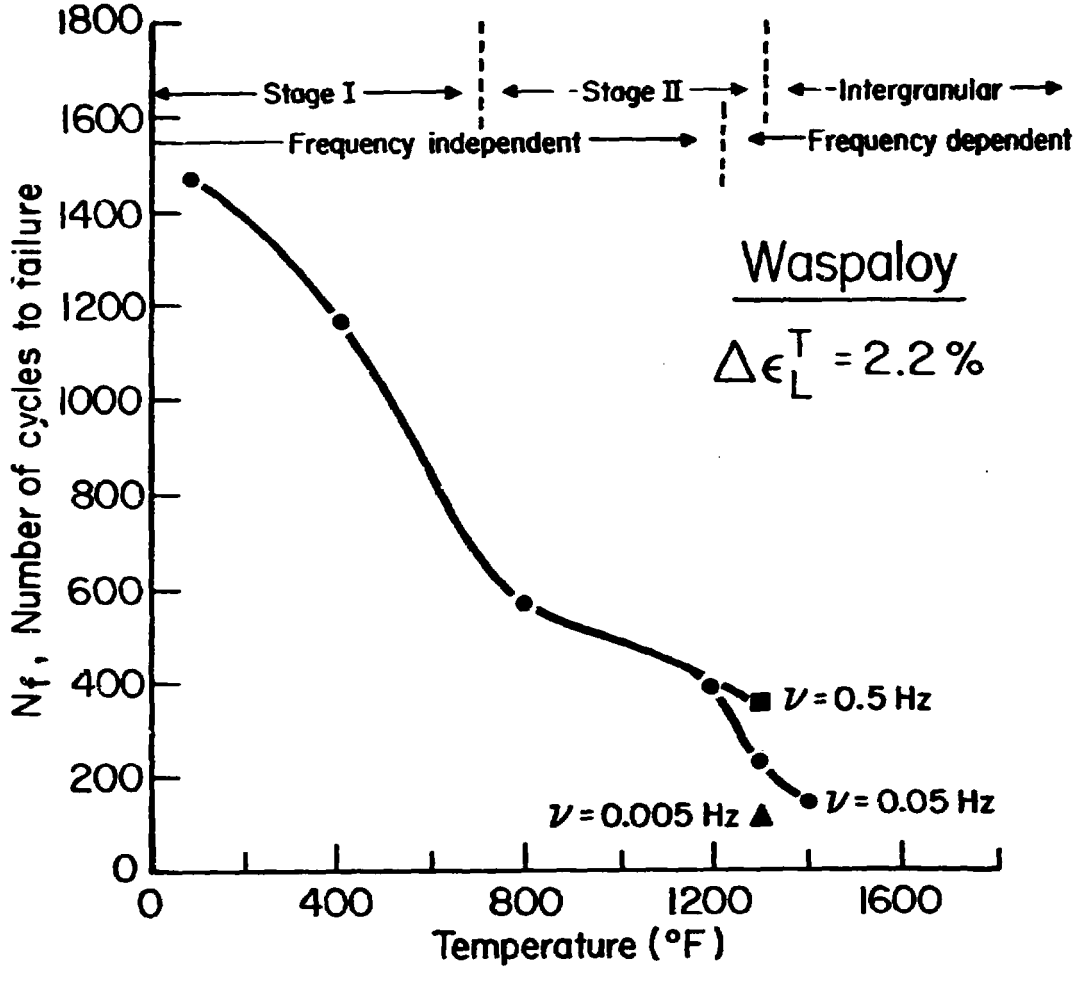

Figure 4. The variation of fatigue lifetime with temperature of Waspaloy.

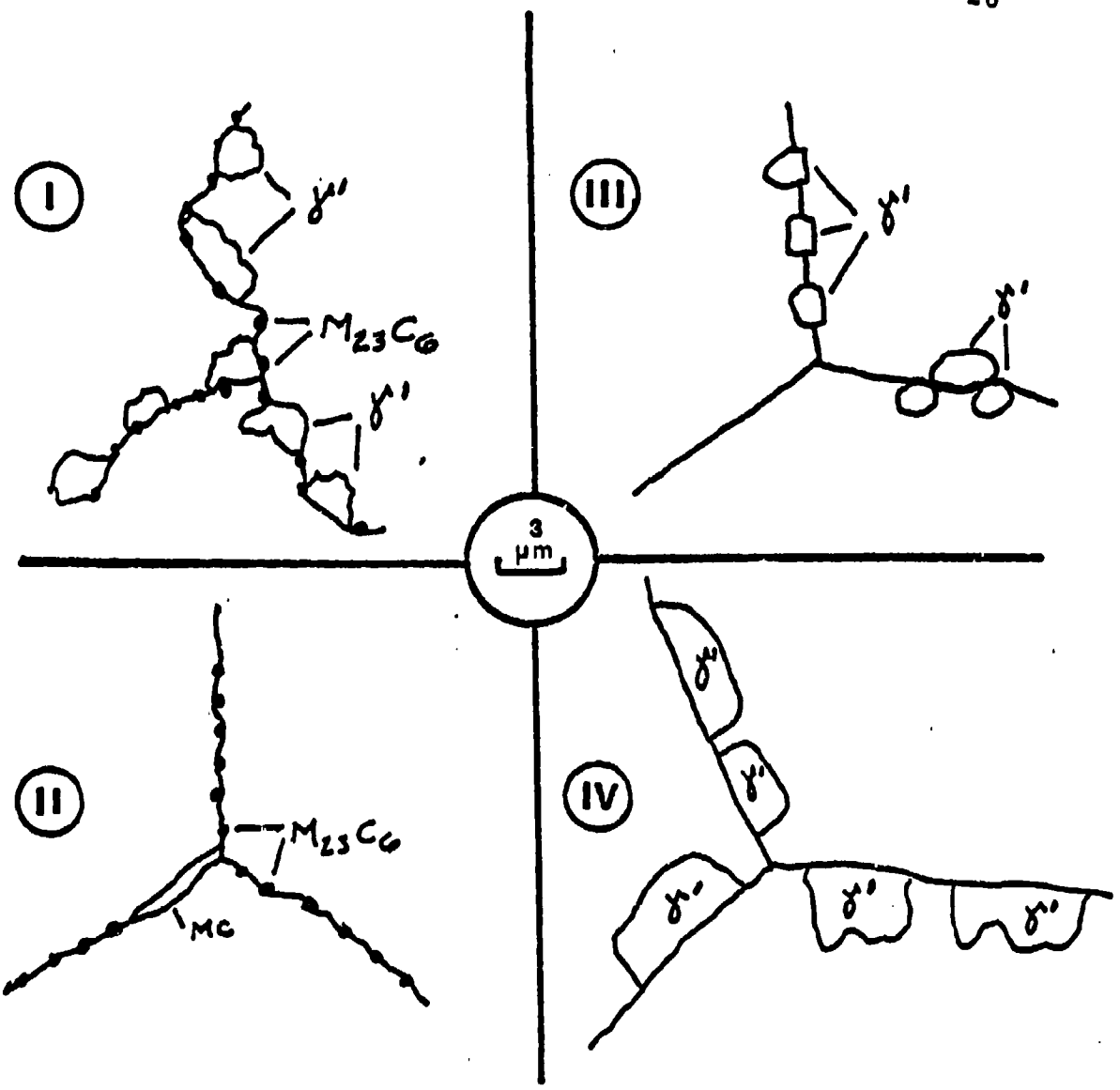

Figure 5. Sketches of low carbon Astroloy grain boundaries.

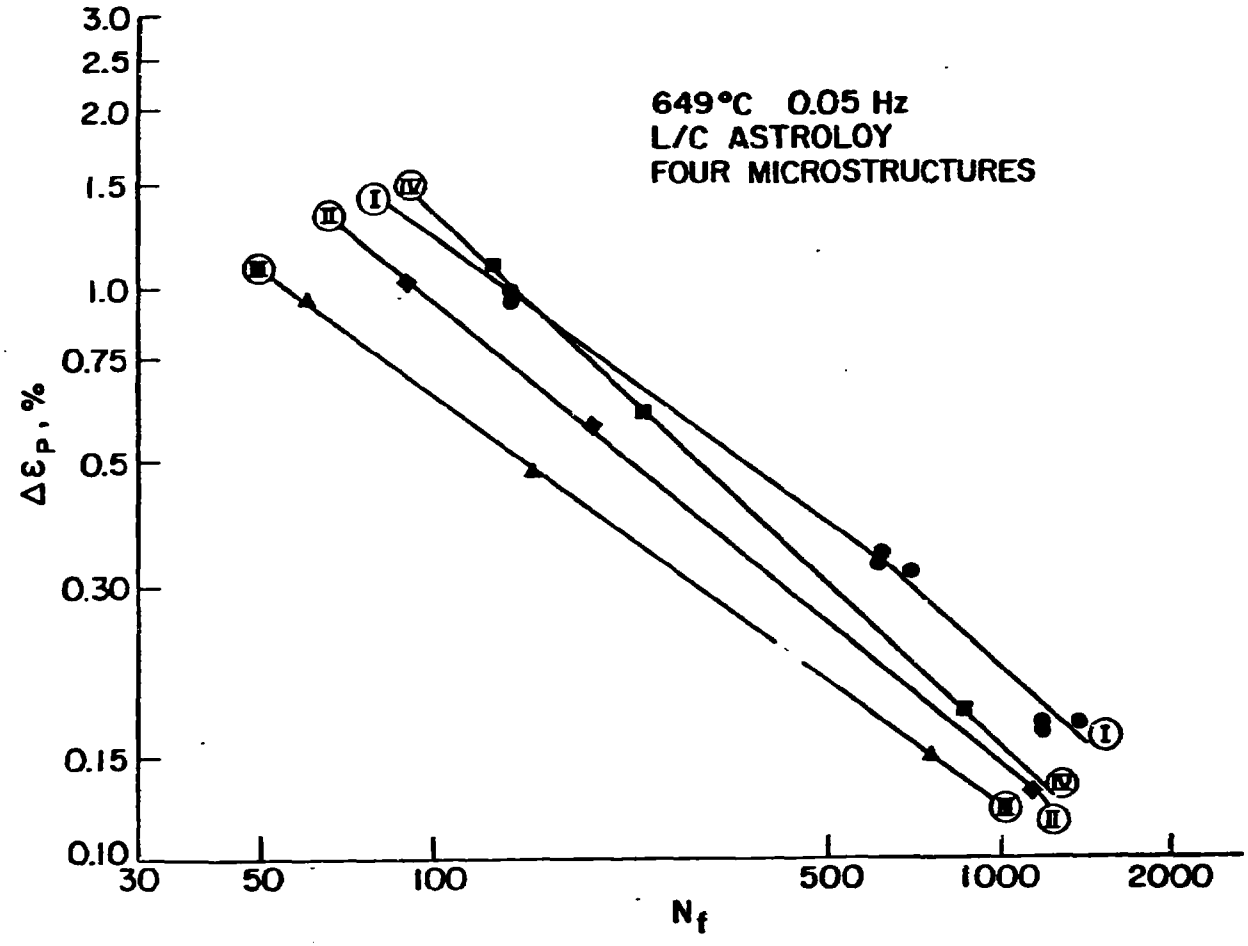

Figure 6. Number of cycles to failure versus plastic strain range for the four microstructures of low carbon Astroloy tested at 649°C and 0.05 Hz.

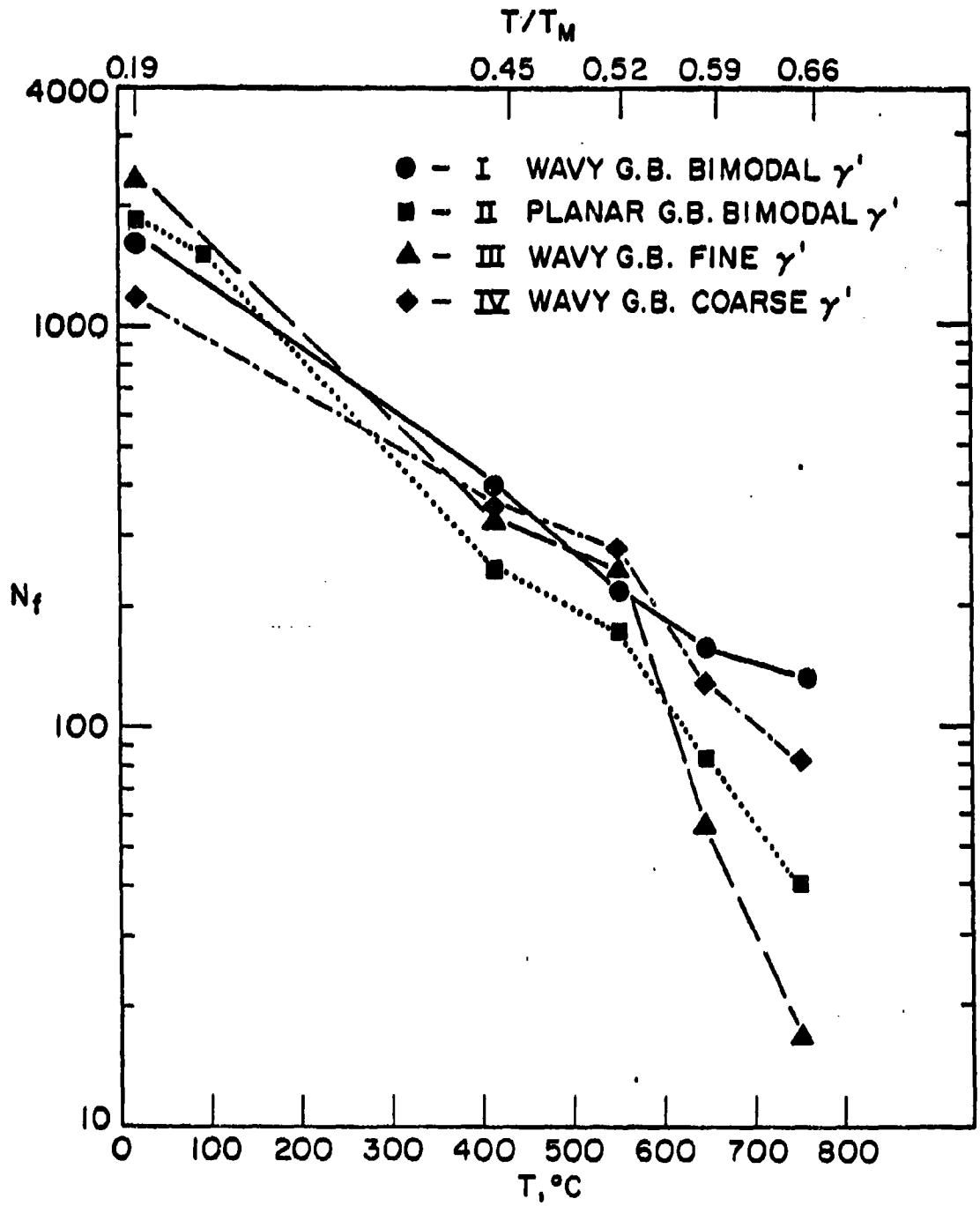

Figure 7. The variation on number of cycles to failure with temperature for the four microstructures of low carbon Astroloy tested at a constant total strain range of 2.2%.

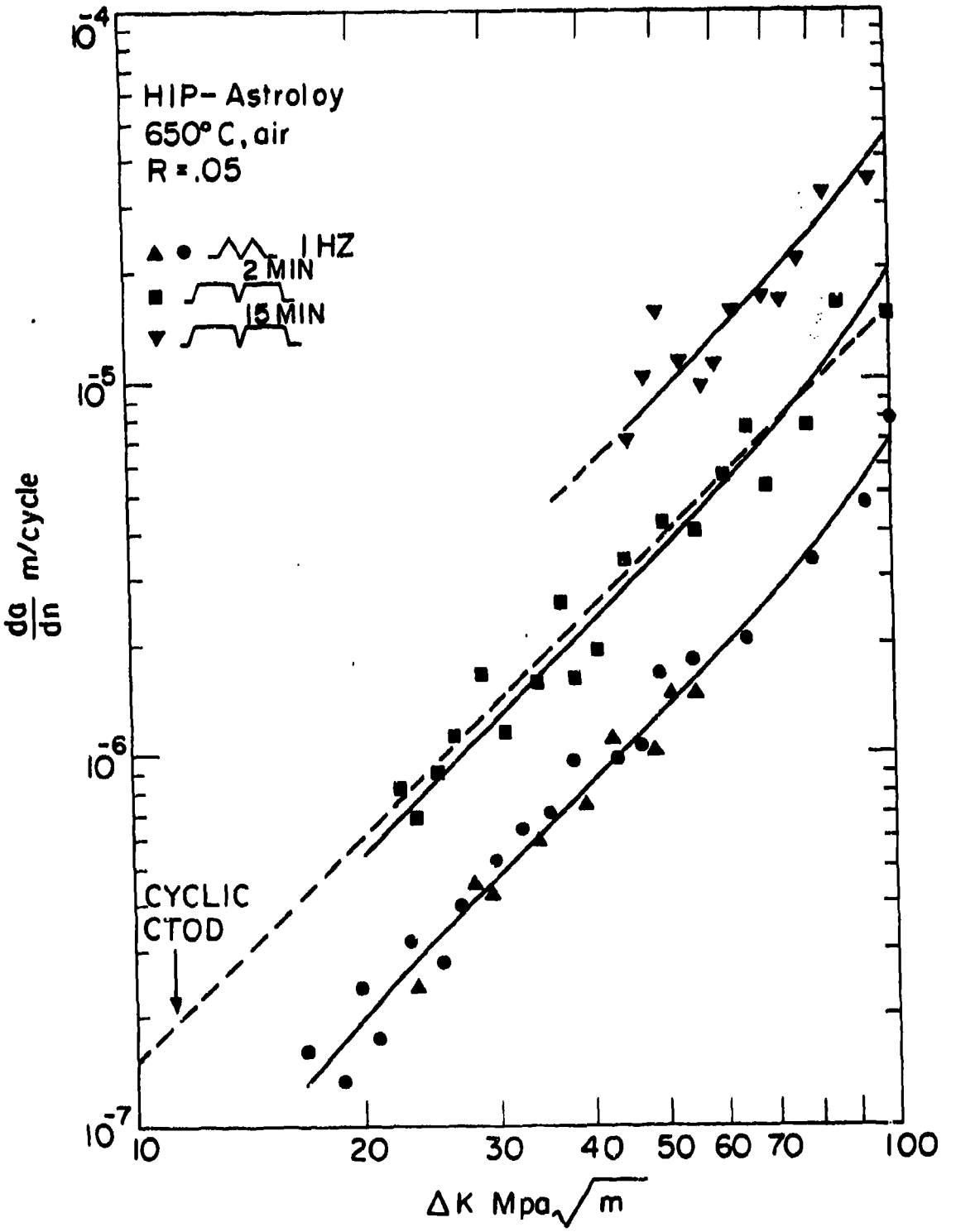

Fig. 8. Fatigue crack growth rates vs ΔK for L/C Astroloy in air, at 650°C.

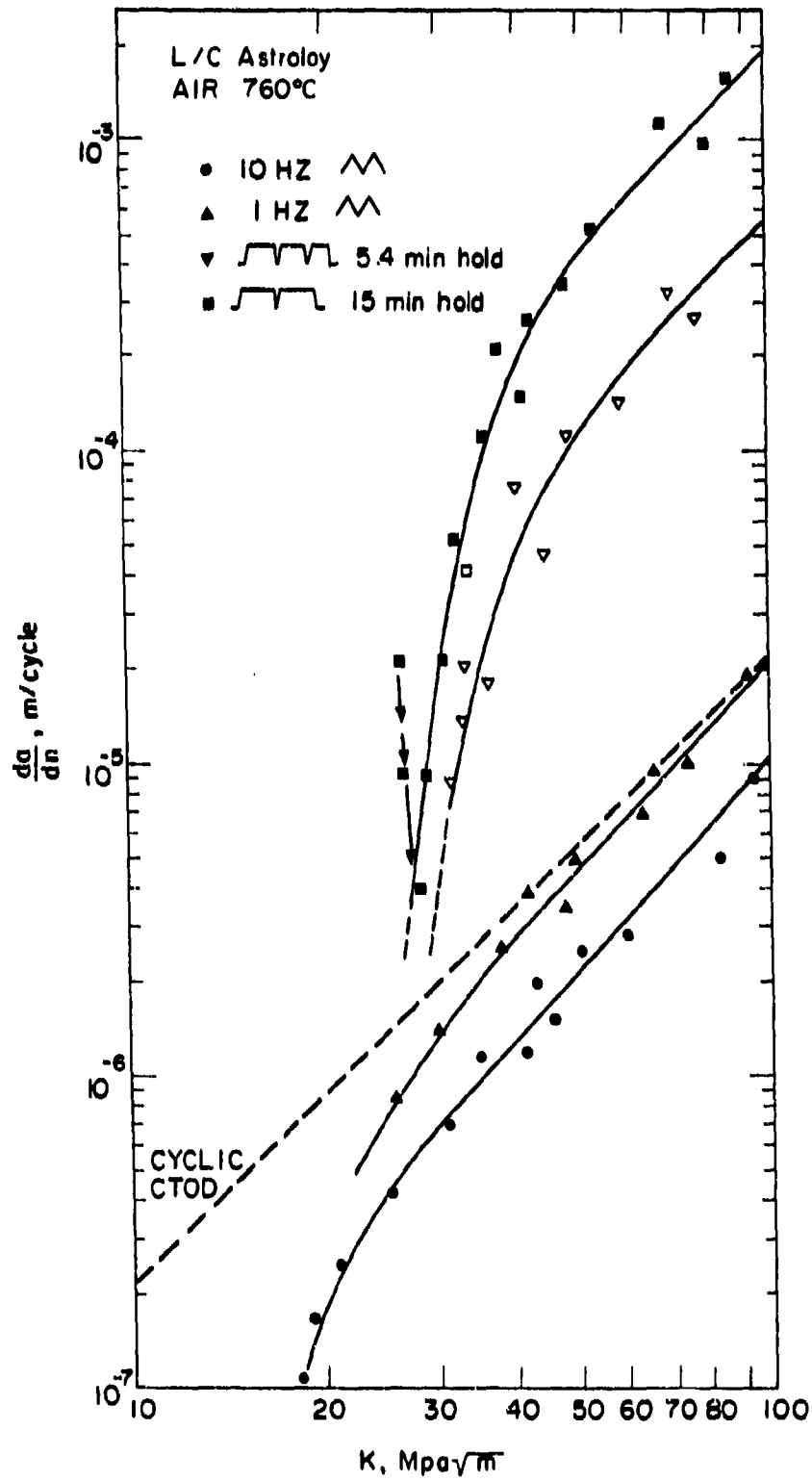

Fig. 9. Fatigue crack growth rates vs ΔK for L/C Astroloy in air, at 760°C.

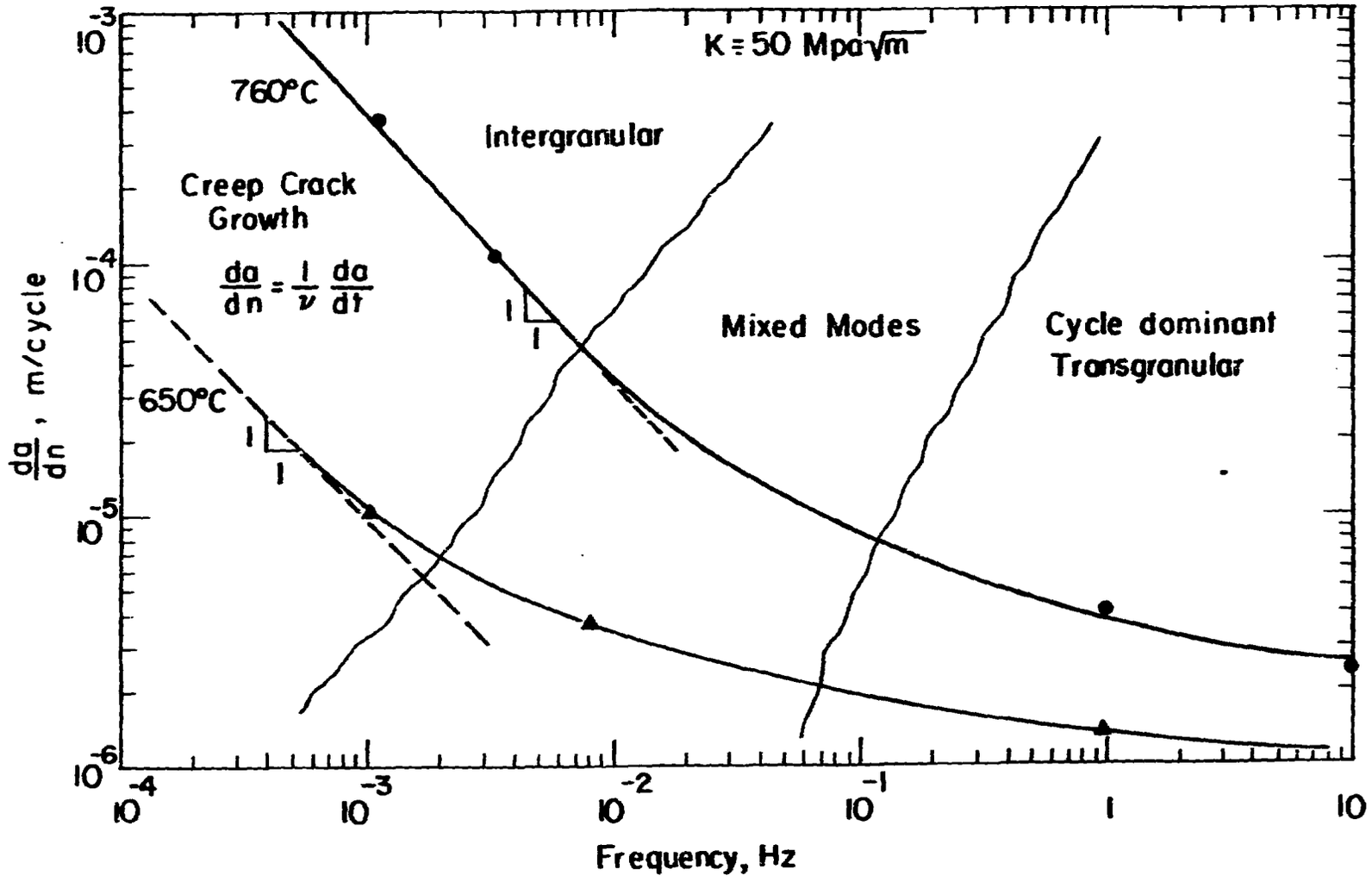

Fig. 10. Fatigue crack growth rates of L/C Astroloy vs frequency and fracture mechanisms at $\Delta K = 50$ MPa$\sqrt{m}$ and 650°C, 760°C.

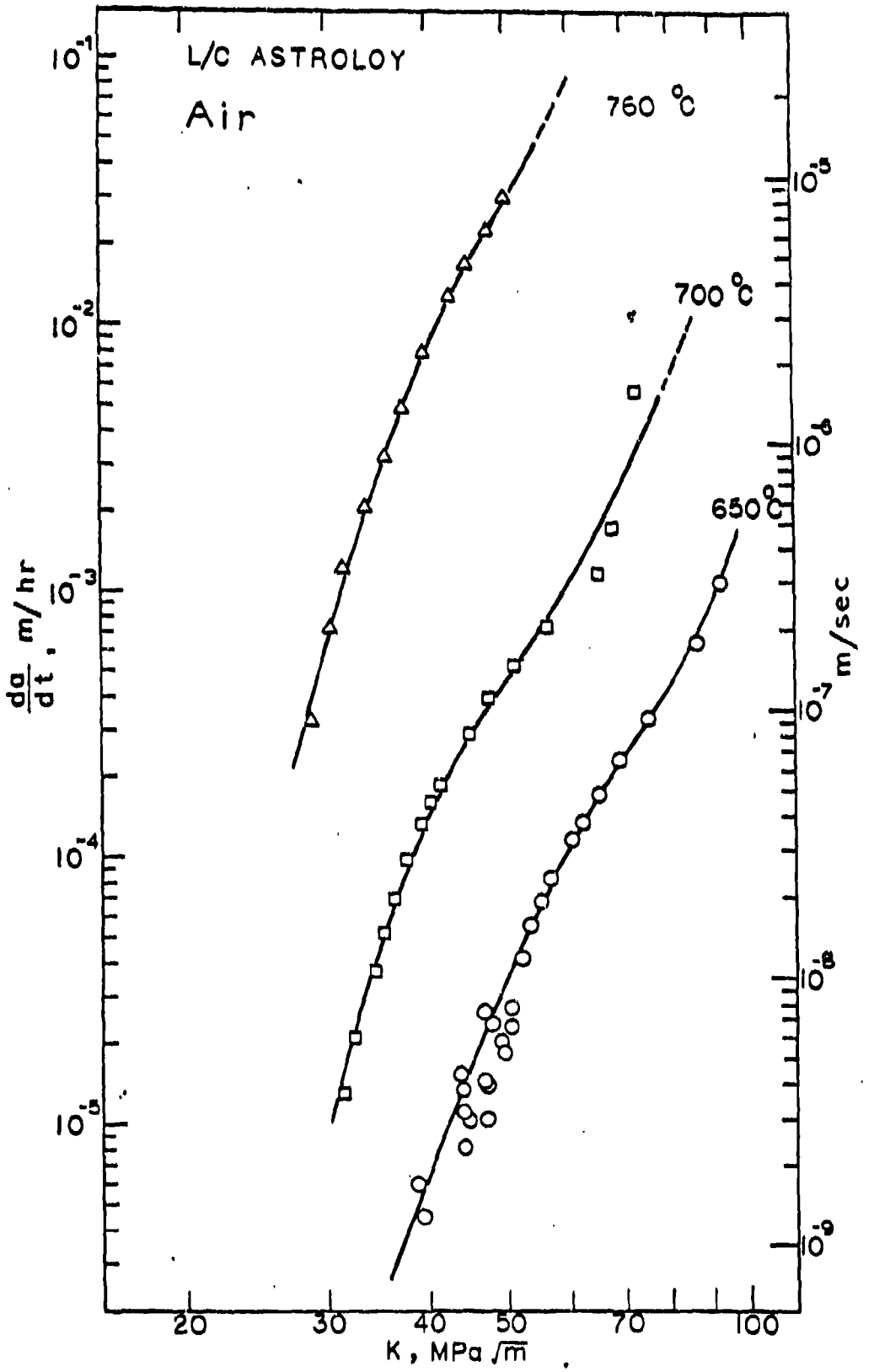

FIGURE 11. CREEP CRACK GROWTH RATES OF LOW CARBON ASTROLOY AT DIFFERENT TEMPERATURES.

Table I - Heat Treatment Program

ALL HIP 1218°C/1000 atm/3 hours

I. WAVY GRAIN BOUNDARY (reference microstructure)

* 1121°C/4 hours/≠AC + 871°C/8 hours/AC

+ 982°C/4 hours/AC + 649°C/24 hours/AC + 760°C/ 8 hours/AC

II. PLANAR GRAIN BOUNDARY (intended structure)

* 1150°C/4 hours/AC + 871°C/ 8 hours/AC

+ 982°C/4 hours/AC + 649°C/24 hours/AC + 760°C/ 8 hours/AC

III. WAVY GRAIN BOUNDARY - FINE γ' (intended structure)

• 1121°C/4 hours/≠≠OQ + 760°C/1 hour/AC

• 1121°C/4 hours/OQ + 760°C/4 hours/AC

* 1107°C/4 hours/OQ + 760°C/4 hours/AC

IV. WAVY GRAIN BOUNDARY - COARSE γ' (intended structure)

• 1121°C/4 hours/AC + 800°C/48 hours/AC

• 1121°C/4 hours/AC + 800°C/216 hours/AC

* 1121°C/4 hours → cool 0.5°C/min to 760°C

---

* selected for LCF evaluation

≠ air cooled

≠≠ oil quenched

TABLE II

Mode of LCF Crack Initiation and Propagation

Temperature °C (°F)	Frequency Hz	Alloy	Mode of Initiation *	Mode of Propagation *
RT	0.04	Waspaloy	I	I
RT	0.05	L/C Astroloy(I)	I	I
		(II)	I	I
		(III)	I	I
		(IV)	I	I
427(800)	0.05	Waspaloy	I	II
		L/C Ast(I)	I	II
		L/C Ast (II)	I	I
		L/C Ast (III)	I	II
		L/C Ast (IV)	I	II
538(1000)	0.05	L/C Ast (I)	I	II
		L/C Ast (II)	I	I+
		L/C Ast (III)	I	I+I
		L/C Ast (IV)	I	II
549(1200)	0.05	Waspaloy	I	II
		L/C Ast (I)	I	II
		L/C Ast (II)	I+IG	I+II
		L/C Ast (III)	IG	I
		L/C Ast (IV)	I	II+I
	0.005	L/C Ast (I)	IG	II+50%I
	0.5	L/C Ast (I)	I	II
	0.5	L/C Ast (II)	I	I
760(1400)	0.05	Waspaloy	I	II+20%I
		L/C Ast (I)	IG	II (after less than 1 grain diameter
		L/C Ast (II)	IG	I
		L/C Ast (III)	IG	I
		L/C Ast (IV)	IG	II

---

* KEY: I - stage I
II - stage II
IG - intergranular